

*Climate of the Past Discussions* is the access reviewed discussion forum of *Climate of the Past*

# Holocene weak summer East Asian monsoon intervals in subtropical Taiwan and their global synchronicity

K. Selvaraj<sup>1</sup>, C.-T. A. Chen<sup>1</sup>, and J.-Y. Lou<sup>2</sup>

<sup>1</sup>Institute of Marine Geology and Chemistry, National Sun Yat-sen University, Kaohsiung 804, Taiwan

<sup>2</sup>Department of Marine Science, Naval Academy, P.O. Box 90175, Tsoying, Kaohsiung, Taiwan

Received: 22 July 2008 – Accepted: 22 July 2008 – Published: 13 August 2008

Correspondence to: K. Selvaraj (kselva8@yahoo.com)

Published by Copernicus Publications on behalf of the European Geosciences Union.

## Weak EAM intervals in Taiwan

K. Selvaraj et al.

[Title Page](#)

[Abstract](#)

[Introduction](#)

[Conclusions](#)

[References](#)

[Tables](#)

[Figures](#)

◀

▶

◀

▶

[Back](#)

[Close](#)

[Full Screen / Esc](#)

[Printer-friendly Version](#)

[Interactive Discussion](#)



## Abstract

CPD

4, 929–953, 2008

Sedimentary total organic carbon and carbon-to-nitrogen ratio records from the sub-alpine Retreat Lake in NE Taiwan reveal four centennial periods (~8–8.3, 5.1–5.7, 4.5–~2.1, and 2–1.6 kyr BP) of relatively reduced summer East Asian monsoon (EAM) precipitation that were superimposed on the insolation-dependent, long-term decreasing monsoon trend during the middle and late Holocene while early Holocene monsoon strength was controlled by glacial boundary conditions. Strikingly, all weak monsoon events correlate with the timings of low sea surface temperature in the tropical Pacific, maxima of hematite stained-grains in the sediments of North Atlantic, reduced formation of North Atlantic Deep Water, and low concentrations of atmospheric methane over Greenland, suggesting a globally well-connected postglacial climate (from ca. 8.6 kyr BP onwards). Persistent linkage of weak summer EAM-tropical Pacific and North Atlantic cooling-reduced global wetland extent during these intervals is believed to be driven by coupled ocean-atmosphere interactions, especially reduced heat and moisture transport and enhanced El Niño-Southern Oscillation in the tropical Pacific, as well as solar activity. Overall similarity of summer EAM with diverse proxy records and their coincidence to abrupt changes witnessed in other paleorecords across the world imply that the centennial-scale reorganizations in the tropical Pacific climate dynamics may have been playing an important role, of course closely in phase with solar variations and North Atlantic climate, in the Holocene summer EAM and, by extension, low-latitude's monsoon instability.

## 1 Introduction

A number of existing high-resolution Holocene's monsoon reconstructions from Indian and Asian domains reveal significant correlation with solar forcing (e.g. Fleitmann et al., 2003; Gupta et al., 2005; Wang et al., 2005). Complement to this, modeling studies demonstrate direct Northern Hemisphere insolation forcing on the African-Asian mon-

## Weak EAM intervals in Taiwan

K. Selvaraj et al.

[Title Page](#)

[Abstract](#)

[Introduction](#)

[Conclusions](#)

[References](#)

[Tables](#)

[Figures](#)

◀

▶

◀

▶

[Back](#)

[Close](#)

[Full Screen / Esc](#)

[Printer-friendly Version](#)

[Interactive Discussion](#)



soons (Kutzbach and Otto-Bliesner, 1982; Joussaume et al., 1999). Though this force explains the long-term monsoon trends in the northern subtropics during the Holocene (e.g. Fleitmann et al., 2007), the number of discrete intervals of weak monsoon and associated abrupt climate changes, for instance ca. 8.2 and 5.4 kyr BP, remain poorly understood. Even though these abrupt monsoon changes in the tropics and subtropics are comparable to quasi-periodic (~1000–1500 yr) cold, dry events in the North Atlantic (Gupta et al., 2003; Porter and Zhou, 2006), their unknown plausible causes and apparent cultural collapses especially during the later Holocene have drawn the tropical climate dynamics as an alternate, albeit promising, climate forcing. Indeed, recent high-resolution studies from the tropical Pacific provide significant evidences that climate change may have been either initiated in or modulated via the tropics (Lea et al., 2000; Stott et al., 2002).

Because of its wide geographic extent, the tropical Pacific is the region of highest heat and moisture flux to the atmosphere and also the hub of activity associated with the El Niño-Southern Oscillation (ENSO) (Cane, 1998; Stott et al., 2002). This region is also the locus of origin for the upper limb of the ocean thermohaline conveyor system, which transports heat and salt to the North Atlantic through surface waters to compensate for North Atlantic Deep Water (NADW) production. In addition, the energetic importance of its equatorial upwelling acts as a dominant carbon dioxide (CO<sub>2</sub>) source to the atmosphere. Despite all these, the role of tropical Pacific forcing on the East Asian monsoon (EAM) and associated climate variability during the Holocene remains poorly implied due primarily to the lack of high-resolution climate records in the high-standing islands of Asia-Oceania (Taiwan, the Philippines, Papua New Guinea, and New Zealand), a major source of salts/nutrients to the western tropical Pacific (WTP) owing to their extremely high erosional but moderate chemical weathering rates (e.g. Selvaraj and Chen, 2006). Furthermore, the dependence of summer EAM precipitation to changes in tropical Pacific sea surface temperature (SST) and NADW variability during the Holocene remains unconstrained in East Asia, but a high-resolution, at least centennial-scale, record of such relationship would pro-

## Weak EAM intervals in Taiwan

K. Selvaraj et al.

[Title Page](#)

[Abstract](#)

[Introduction](#)

[Conclusions](#)

[References](#)

[Tables](#)

[Figures](#)

◀

▶

◀

▶

[Back](#)

[Close](#)

[Full Screen / Esc](#)

[Printer-friendly Version](#)

[Interactive Discussion](#)



vide insight into EAM-tropical Pacific-North Atlantic climate dynamics. Here we present high-resolution (<20 years in some intervals of mid-Holocene) lacustrine geochemical evidences for four, mostly in centennial-scale, intervals (~8–8.3, 5.1–5.7, 4.5–2.1 and 2–1.6 kyr BP) of weakened summer EAM precipitation, synchronous to climate and environmental changes in other parts of the world including Southern Hemisphere, from NE Taiwan during the postglacial period (from ~8.6 kyr BP to the present) of Holocene. Our study also demonstrates weak summer EAM-tropical Pacific-NADW linkage around these time periods that appears to be influenced by the climate dynamics associated with the tropical Pacific, especially heat and moisture transport and El Niño, in phase with the changes in solar activity and North Atlantic climate.

## 2 Area, materials and methods

Taiwan's weather and climate are primarily controlled by the EAM which is formed as a result of thermal difference between the Asian landmass and the tropical Pacific with an additional thermal and dynamic trigger of Tibetan Plateau. In the perspective of climate, the summer EAM is crucial because it regulates global atmospheric circulation through heat and moisture transport from the warmest part of the tropical ocean, the West Pacific warm pool (WPWP), across the equator to extratropics. The hydrologically closed subalpine Retreat Lake is located (24°29'30" N, 121°26'15" E; 2230 m a.s.l.) directly on the route of moisture-laden, southeasterly down-winds of summer EAM from the WTP and close to the main axis of Kuroshio Current (Fig. 1), a major western boundary current that transports a large volume of warm, salty seawater from WTP to northern North Pacific. The modern lake catchments have two distinct seasons: a warm, wet season during the Northern Hemisphere summer (May to September) when the intertropical convergence zone (ITCZ) shifts northward with the development of stronger summer monsoon and a cool, dry season during the boreal winter (October to April) when the Siberian high establishes a strong anticyclone on the Tibetan Plateau and ITCZ migrates to a southern position with the enhancement of winter mon-

CPD

4, 929–953, 2008

## Weak EAM intervals in Taiwan

K. Selvaraj et al.

[Title Page](#)

[Abstract](#)

[Introduction](#)

[Conclusions](#)

[References](#)

[Tables](#)

[Figures](#)

[◀](#)

[▶](#)

[◀](#)

[▶](#)

[Back](#)

[Close](#)

[Full Screen / Esc](#)

[Printer-friendly Version](#)

[Interactive Discussion](#)



soon. These characteristics make the area as an ideal site to study summer monsoon fluctuations including the effect of tropical Pacific heat transport and, therefore, the role of Kuroshio on the East Asian climate. The site experiences the mild mean annual temperature of 12°C and high mean annual precipitation of ~3000 mm; as a result, the 5 modern freshwater lake is surrounded by thick subtropical vegetation with dominant occurrence of *Cyclobalanopsis* and *Quercus*.

We generated an ~10.3 calendar kilo years (kyr) old record of total organic carbon (TOC) and carbon<sub>organic</sub> to nitrogen<sub>total</sub> (C/N) ratio by sampling a 1.7 m long sediment core at contiguous 0.5 and 1 cm intervals from Retreat Lake, providing a high-resolution 10 variations in the summer EAM intensity in subtropical Taiwan. The content of TOC and C/N ratio in lacustrine sediments are valuable indicators of monsoon changes because climate, nature of lake catchments vegetation (C<sub>3</sub> versus C<sub>4</sub>), and lake morphology largely control these parameters (e.g. Meyers and Lallier-Vergès, 1999). Since the lake 15 is situated directly on the moisture-carrying southeasterly down-winds of EAM from the WTP, higher contents of TOC and C/N ratio are indicative of vascular plants dominance and, in turn, strong summer monsoon (Selvaraj et al., 2007). The sediments contained only traces of inorganic carbon and nitrogen and therefore quantities of organic carbon and nitrogen are equal to the amounts of total carbon and nitrogen. Both parameters 20 were analyzed mostly in all samples ( $n=202$ ) with LECO CHN-932 instrument using appropriate combustion temperature as described in Lou and Chen (1997).

Sediment chronology is based on 8 accelerator mass spectrometry (AMS) and 2 conventional <sup>14</sup>C dates of bulk organic matter, all uncorrected dates converted to calendar years as detailed in Selvaraj et al. (2007). The linearly interpolated calendar age-depth model shows highly variable sedimentation rate with a Holocene mean of 25 16.8 cm/kyr (Fig. 2). The average age interval per studied sample is ~45 years ranging from 2 to 98 years/cm sedimentation except in the late Holocene lake desiccation interval ca. 4.5–2.1 kyr BP, the same is very high, i.e. ~790 years/cm, because of starvation of organic-inorganic materials input (Figs. 2 and 3). The time series of TOC and C/N ratio of Retreat Lake are compared with (i) insolation data at 30° N averaged from June

## Weak EAM intervals in Taiwan

K. Selvaraj et al.

[Title Page](#)

[Abstract](#)

[Introduction](#)

[Conclusions](#)

[References](#)

[Tables](#)

[Figures](#)

◀

▶

◀

▶

[Back](#)

[Close](#)

[Full Screen / Esc](#)

[Printer-friendly Version](#)

[Interactive Discussion](#)



to August (Berger and Loutre, 1991), (ii) atmospheric concentrations of CO<sub>2</sub> recorded in Taylor Dome ice core from Antarctica (Indermühle et al., 1999); (iii) percentage of *Globigerina bulloides* in Hole 732A from the Arabian Sea (Gupta et al., 2005); (iv) cave stalagmite  $\delta^{18}\text{O}$  values of Indian summer monsoon from southern Oman (Fleitmann et al., 2003); (v) tree-ring  $\Delta^{14}\text{C}$  residuals record of past solar variability (Stuiver et al., 1998); (vi) Holocene record of faunal Mg/Ca-derived tropical Pacific SST from core MD81 (Stott et al., 2004); (vii) percentage of hematite-stained grains in core V29-191 from the North Atlantic (Bond et al., 2001); (viii)  $\delta^{13}\text{C}$  data of benthic foraminifera, an established proxy for NADW variability, from the sediments of ODP site 980 in the sub-polar northeastern Atlantic (Oppo et al., 2003); and (ix) atmospheric concentrations of methane (CH<sub>4</sub>) recorded in GRIP ice core from Greenland (Blunier et al., 1995).

### 3 Results and discussion

#### 3.1 Long-term Holocene summer EAM trend

Because the lake catchments vegetation exerts direct control on the contents of TOC and C/N ratio in the subalpine regions of Taiwan, we interpret the variations of these two parameters as indicators of amount of summer EAM precipitation, with higher (lower) values indicating wetter (drier) conditions (Selvaraj et al., 2007). Consequently, the TOC and C/N ratio records (Fig. 3a and b) show rapid increase at  $\sim 8.6$  kyr BP due mainly to an abrupt postglacial strengthening and increase of summer EAM as a result of northward migration of ITCZ in response to summer solar insolation. A marked change from organic-poor to -rich, peaty sediments (TOC – 2.1 to 44%; C/N – 9 to 31) is further testimony of the sudden expansion of vascular plant (deep-rooted C<sub>3</sub>) biomass (Fig. 3b). The strong, negative relationship between TOC, a proxy for summer monsoon strength in Taiwan, and insolation evident prior to 8.6 kyr BP suggests that the strength of summer EAM during the early Holocene was largely controlled by glacial boundary conditions presumably Tibetan Plateau snow cover, North Atlantic

#### Weak EAM intervals in Taiwan

K. Selvaraj et al.

[Title Page](#)

[Abstract](#)

[Introduction](#)

[Conclusions](#)

[References](#)

[Tables](#)

[Figures](#)

[◀](#)

[▶](#)

[◀](#)

[▶](#)

[Back](#)

[Close](#)

[Full Screen / Esc](#)

[Printer-friendly Version](#)

[Interactive Discussion](#)



and tropical Pacific SSTs, and lowered atmospheric CO<sub>2</sub>. This interpretation is very consistent with similar relationship shown by the Indian summer monsoon record (reduced *G. bulloides* abundance ~9.8–8.6 kyr BP) with insolation (yellow bar in Fig. 3) and positive correlation of oxygen isotope values from Oman speleothem with Greenland air temperatures (figure not shown) between ~10.3 and 8 kyr BP (Fleitmann et al., 2003). Visual comparison of our time series data with  $\Delta^{14}\text{C}$  residuals record, which largely reflects variations in solar activity, in general, shows weak solar irradiance (higher  $\Delta^{14}\text{C}$ ) before 8.6 kyr (Fig. 3d), suggesting that the prevailed low solar output perhaps in phase with glacial boundary conditions inferred here would have delayed the development and advance of summer monsoon in Taiwan while associated low air temperature would also have decreased the export of water vapor to the atmosphere (An et al., 2000). Nonetheless, the clear representation of Indian summer monsoon increase evident at ~9.7 kyr BP in the *G. bulloides* record is not obvious in our summer EAM records due essentially to the resolution of samples/data missing between roughly 9.6 and 10.1 kyr BP (Fig. 3a).

In contrast to the observed negative summer EAM-insolation relationship, our geochemical records show a strong visible coincidence with insolation from ~8.6 kyr BP onward, indicating that long-term decrease in postglacial monsoon intensity depends on orbitally-induced summer solar insolation (Fig. 3a). Interestingly, a long-term decrease in the contents of TOC and C/N ratio, proxies for lake's catchments vegetation and, in turn subtropical vegetation, due to diminished summer EAM precipitation from ca. 7.7 kyr BP onward visually corresponds to long-term increasing trend of atmospheric CO<sub>2</sub> concentrations recorded in ice core from Taylor Dome, Antarctica (Indermühle et al., 1999) (Fig. 3b). This inverse relationship suggests that the middle to late Holocene decrease of insolation-controlled low-latitude's monsoon strength, including East Asian, Indian, and South American monsoons, and associated reduction in tropical and subtropical vegetation cover could be plausible factors that are responsible for gradual CO<sub>2</sub> increase for the past ~8 kyr. Organic-rich peaty sediments with high TOC values and C/N ratio as a consequence of stronger summer monsoon that

## Weak EAM intervals in Taiwan

K. Selvaraj et al.

[Title Page](#)

[Abstract](#)

[Introduction](#)

[Conclusions](#)

[References](#)

[Tables](#)

[Figures](#)

◀

▶

◀

▶

[Back](#)

[Close](#)

[Full Screen / Esc](#)

[Printer-friendly Version](#)

[Interactive Discussion](#)



developed during the Holocene optimum between ~8.6 and 4.5 kyr BP in NE Taiwan concur with the warmer but less humid interval (8–4 kyr BP) with abundant subtropical vegetation inferred from a subalpine pollen sequence when the forests were more extensive in central Taiwan (Liew et al., 2006). Considering the fact that this interval 5 was the time of a Holocene precipitation optimum in China (Porter, 2000), we could correlate our records with Loess Plateau stratigraphy by matching roughly the interval (~8.6–4.5 kyr BP) of stronger summer monsoon with S0 paleosol (9.5 and 5.5 kyr BP) while later Holocene dry climate and lake desiccation in our site correspond to the timings of the formation of Potou Loess (~5.5–0 kyr BP) (Porter and Zhou, 2006). Based 10 on this tentative correlation as well as previous comparison of warm, wet mid-Holocene in NE Taiwan with warm, dry Megathermal in Inner Mongolia (Chen et al., 2003), we suggest that Holocene optimum conditions, either in terms of maximum precipitation or temperature or combination of these two variables, prevail probably between around 9 and 4.5 kyr BP in China.

### 15 3.2 Weak summer EAM intervals in Taiwan

Very interestingly, our proxy records show four weak summer EAM events of relatively larger in amplitude and longer in duration, mostly in centennial-scale, at around 8.3–8, 5.7–5.1, 4.5–2.1, and 2–1.6 kyr BP during the postglacial period of Holocene (grey bars in Fig. 3) when the Siberian High was probably more active because such a condition 20 in SE Asia normally reduces the summer monsoon and strengthens the boreal winter precipitation. It has been demonstrated recently that abrupt centennial-scale changes in Asian monsoon intensity during the Holocene were correlated with solar activity (Gupta et al., 2005; Wang et al., 2005). To know the Sun-EAM link in Taiwan, we therefore combined our unsmoothed time series with  $\Delta^{14}\text{C}_{\text{residuals}}$ , which largely reflects atmospheric solar activity (Stuiver et al., 1998). Some of the weak monsoon intervals 25 represented by relatively low contents of TOC and C/N ratios appear to correlate with weaker solar winds and reduced irradiance as indicated by higher  $^{14}\text{C}$  production rate (small bars in Fig. 3d), suggesting that second order variations in summer EAM

## Weak EAM intervals in Taiwan

K. Selvaraj et al.

[Title Page](#)

[Abstract](#)

[Introduction](#)

[Conclusions](#)

[References](#)

[Tables](#)

[Figures](#)

◀

▶

◀

▶

[Back](#)

[Close](#)

[Full Screen / Esc](#)

[Printer-friendly Version](#)

[Interactive Discussion](#)



precipitation and related lake catchments vegetation changes were triggered by weak solar activity. Based on a close relationship between events of vegetation change in central Taiwan and another cosmogenic nuclide,  $^{10}\text{Be}$ , analogous implications of sun-monsoon link were also made recently (Liew et al., 2006). All the four intervals of monsoon minima, within the dating errors of individual chronologies, strikingly coincide with low SST in the tropical Pacific (Stott et al., 2004), maxima of hematite in the sediments of the North Atlantic (Bond et al., 2001), low  $\delta^{13}\text{C}$  values of benthic foraminifera, *Cibicidoides wuellerstrofi*, reduced contribution of NADW (Oppo et al., 2003), and low concentrations of atmospheric  $\text{CH}_4$  over Greenland (Blunier et al., 1995) (Fig. 3).

### 10 3.2.1 8.3–8 kyr BP event

The event centered at  $\sim 8.17$  kyr BP closely correlates to the “8.2-kyr cold event” recorded in Greenland ice cores (e.g. Alley et al., 1997), and numerous marine and terrestrial proxy records in the North Atlantic region (deMenocal et al., 2000; McDermott et al., 2001), and also coincides with a long-term, modestly declining  $\text{CO}_2$  trend recognized in the Taylor Dome record (Fig. 3b). Although this climatic instability is strongly connected to a brief episode of massive release ( $5.1 \text{ Sv}$ ;  $1 \text{ Sverdrup} = 1 \times 10^6 \text{ m}^3 \text{ s}^{-1}$ ) of meltwater associated with the final demise of Laurentian ice sheet, the chronologically well established deglacial period 8.8–7.5 kyr BP of this event (Barber et al., 1999), within dating error, seems to closely correlate with abrupt, postglacial strengthening as well as maximum of summer EAM between  $\sim 8.6$  and 7.7 kyr BP in subtropical Taiwan (Fig. 3). Given the fact that monsoons are the most efficient means for inter-hemispheric vapor/latent heat transport, this correlation perhaps implies the conceivable link between insolation controlled summer EAM system and prominent Northern Hemisphere cold spell. This inference is further supported by increased heat transport from the tropics to extratropics ca. 9–8.5 kyr BP, which also just predate this event, by warm surface currents such as the Kuroshio in the WTP (Jian et al., 2000) and the Loop Current in the North Atlantic (Poore et al., 2003). Besides, Barber et al. (1999) inferred from the pattern of the 8.2 kyr cooling event that heat transport from the ocean

## Weak EAM intervals in Taiwan

K. Selvaraj et al.

[Title Page](#)

[Abstract](#)

[Introduction](#)

[Conclusions](#)

[References](#)

[Tables](#)

[Figures](#)

◀

▶

◀

▶

[Back](#)

[Close](#)

[Full Screen / Esc](#)

[Printer-friendly Version](#)

[Interactive Discussion](#)



to the atmosphere was reduced in the North Atlantic. Considering the cascade of all these events starting from insolation peak at 65° N around 9 kyr BP, we speculate that low-latitude summer monsoon and associated vapor/latent heat transfer might be another possible trigger for melting of Laurentian ice sheet around 8.47 kyr BP which was 5 responsible for the 8.2 kyr cold event (Barber et al., 1999). Recent critical review of the 8.2 kyr cooling event by Rohling and Pälike (2005) favorably highlights that many proxy records (90%) around the globe show a well-dated onset of climatic deterioration well before 8.4 kyr BP including summer monsoon reduction in low-latitudes largely occurring between roughly 8.5 and 8.1 kyr BP.

### 10 3.2.2 5.7–5.1 kyr BP event

The reduced summer EAM revealed prominently by strong troughs in TOC and C/N ratio records (Fig. 3) centered at ~5.4 kyr BP closely correlates to the termination timing (5.5 kyr BP) of African humid period and coincides with abrupt decrease of moisture availability in tropical Africa (deMenocal et al., 2000). This event further corresponds 15 to a sharp drop in Asian monsoon intensity in the regions between eastern Africa and northeast China (Morrill et al., 2003), clear drop in lake level in central Tibet (Morrill et al., 2006), and rapid climate change revealed by the compilation of Holocene climate records (Mayewski et al., 2004). All these low-latitude's climate changes ca. 5.5–5 kyr BP closely correspond to the establishment of modern frequencies of the ENSO 20 (Sandweiss et al., 1996; Rodbell et al., 1999) while drier condition over the Cariaco Basin commenced due to southward migration of Atlantic ITCZ (Haug et al., 2001). Since the ENSO results from instabilities in the coupled ocean-atmosphere that drives interannual shifts in oceanographic and atmospheric variables throughout the Pacific (Gagan et al., 2004), the covariance among these events thus strongly invokes the 25 active involvement of nonlinear ocean-atmosphere interactions, most likely between ENSO and southward migrating ITCZ in the tropical Pacific, during the later Holocene. This interaction probably reduces the seasonality of summer monsoon when compared to its relatively longer seasonality before 4.5 kyr BP, especially during the interval of

## Weak EAM intervals in Taiwan

K. Selvaraj et al.

[Title Page](#)

[Abstract](#)

[Introduction](#)

[Conclusions](#)

[References](#)

[Tables](#)

[Figures](#)

[◀](#)

[▶](#)

[◀](#)

[▶](#)

[Back](#)

[Close](#)

[Full Screen / Esc](#)

[Printer-friendly Version](#)

[Interactive Discussion](#)



Holocene optimum between roughly 10.5 and 4.5 kyr BP, when the ITCZ was in its northernmost position within the Holocene. In fact, comparable and correlative evidences are seen to be widespread in Southern Hemisphere where initiation of Neoglacial phase was inferred from the advances of mountain glaciers in South America and New Zealand between ~5.4 and 4.9 kyr BP (Porter, 2000). Around the same time, Hodell et al. (2001) found abrupt cooling of SST, expansion of sea ice, and increased icerafted debris accumulation in a sediment core from the subantarctic South Atlantic. A widespread global cooling and contrasting hydrological changes apparent from numerous other climatic records across the world ca. 5.5–5 kyr BP, the time period again exactly marks the Hypsithermal-Neoglacial transition elsewhere (e.g. Steig, 1999) (dotted line in Fig. 3), suggesting a major global-wide abrupt climate reversal and environmental change.

Based on calcite isotope records of speleothem, Fleitmann et al. (2007) discussed that the middle to late Holocene Asian monsoon weakness was a gradual, but not an abrupt, process in phase with a continuous southward migration of ITCZ. Their cave  $\delta^{18}\text{O}$  record of Indian summer monsoon (Fig. 3c), similar to  $\delta^{18}\text{O}$  record, a temperature proxy, in Greenland ice cores (Stuiver and Grootes, 2000), did not support the 5.5 kyr BP event. The evidences submitted above however indicate that 5.5–5 kyr BP event was probably one of the largest, centennial-scale events within the Holocene when heat flux to atmosphere was greatly reduced as indicated by longest duration (6.1 to 5 kyr BP) of reduced NADW formation (Oppo et al., 2003) (Fig. 3f) while O'Brien et al. (1995) inferred an extreme winter-like condition through statistical analysis of paleochemical indicators from GISP2. These are again consistent with the largest amount of hematite stained-grains in the North Atlantic (Fig. 3e) and correspond to a period (5.6–5.2 kyr BP) of weaker solar activity as indicated by a  $\Delta^{14}\text{C}$  maximum in the atmosphere (Fig. 3d), indicating a prominent North Atlantic cooling. The former phenomenon, i.e. the weakest NADW production, seems to be one of the causes for the lowest methane recorded in the Greenland ice core during this time interval as reduced NADW formation weakens the heat transport to the atmosphere and, there-

## Weak EAM intervals in Taiwan

K. Selvaraj et al.

[Title Page](#)

[Abstract](#)

[Introduction](#)

[Conclusions](#)

[References](#)

[Tables](#)

[Figures](#)

◀

▶

◀

▶

[Back](#)

[Close](#)

[Full Screen / Esc](#)

[Printer-friendly Version](#)

[Interactive Discussion](#)



fore, Northern Hemisphere wetland extent (Fig. 3f). These inferences further insinuate that abrupt climate changes associated with strong positive feedbacks which link tropical/subtropical vegetation, albedo, and precipitation may not be explained by  $\delta^{18}\text{O}$  variations of either tropical speleothem or polar ice core. Although this perception needs to be validated with more high-resolution tropical data, the near synchrony and abruptness of all the climate changes observed/cited reveal a plausible link among East Asia, tropical Pacific, North Atlantic, and Greenland that involved a nonlinear response probably of strong ENSO-low latitude's monsoon interaction to gradual changes in Northern Hemisphere insolation.

### 10 3.2.3 Lake desiccation (4.5–~2.1 kyr BP) event

A wide interval of weak summer EAM and subsequent lake desiccation as well as sedimentation hiatus at ~4.5 to 2.1 kyr BP (Fig. 3a) are suggestive of dry climatic conditions in the late Holocene. Low lake levels in China (Wei and Gasse, 1999), India (Enzel et al., 1999), and East and West Africa (Street-Perrott and Perrott, 1990) due to 15 an effect of weakened summer monsoon were noted mostly within this interval. Consistent to sedimentation hiatus in NE Taiwan, the cores collected from Ahung Co Lake in central Tibet do not contain sediment for the last 4 kyr (Morrill et al., 2006) and Liu et al. (1998) observed the minimum pollen concentrations (50 grains/liter) between 4.8 and 2.7 kyr BP in Dunde ice core due to lower effective moisture and thus weakened 20 summer monsoon. Pertinent coincidence of this time interval to the archeological evidences such as the collapse of Neolithic culture all over China (Wu and Liu, 2004) and the collapse of Akkadian empire (Weiss et al., 1993) as an effect of increase in Mesopotamian aridity (Cullen et al., 2000), indicate weakness perhaps failure of summer monsoon across the low-latitude regions.

25 It has been shown through instrumental and proxy reconstructions that SST and rainfall in tropics are intimately related and because of the nonlinear relationship between SST and heat transfer to the atmosphere (e.g. Palmer and Madsfield, 1984), even small changes in the tropical SST (0.5–1°C) can have significant effects on the patterns

## Weak EAM intervals in Taiwan

K. Selvaraj et al.

[Title Page](#)

[Abstract](#)

[Introduction](#)

[Conclusions](#)

[References](#)

[Tables](#)

[Figures](#)

[◀](#)

[▶](#)

[◀](#)

[▶](#)

[Back](#)

[Close](#)

[Full Screen / Esc](#)

[Printer-friendly Version](#)

[Interactive Discussion](#)



of rainfall, storm tracks, and intensities by affecting the overall general atmospheric circulation (e.g. Rind, 1990). Strikingly, the longest interval of late Holocene weak summer monsoon in subtropical Taiwan and number of Neolithic cultural collapses in China (Wu and Liu, 2004) corresponds to a sharp decrease in faunally-reconstructed SST, which is an indication of intense El Niño, between ~5 and 2 kyr BP in the WTP (Fig. 3e). This correlates with reduced meridional heat transport from tropical to northern North Pacific as inferred from a substantial decrease of indicator species of warm Kuroshio, *Pulleniatina obliquiloculata*, in the sediment cores of Okinawa Trough between 4.5 and 2.7 kyr BP (e.g. Jian et al., 2000). This “*P. obliquiloculata* minimum event” was also recorded in the South China Sea between 4.9 and 2.9 kyr BP (Wang et al., 1999) while Wei et al. (1997) observed better preservation of nannofossil assemblages and a drop in SST, coherent with the WTP, ~5–3 kyr BP, indicating reduced heat transport from the WTP to its marginal seas as well and relatively cooler Indo-Pacific warm pool. Variable and cooler SST evident in tandem between 5 and 2 kyr BP indicate decreased transport of Caribbean surface waters by warm Loop Current into the western Gulf of Mexico (Poore et al., 2003). These events correlate with the past temperatures reconstructions from GRIP borehole that showed temperature decrease, again comparable to WTP, between 5 and 2 kyr BP (Dahl-Jensen et al., 1998) and coincides with the biological indications of widespread cooling of surface waters in the Atlantic (deMenocal et al., 2000) and Indian Oceans (Bard et al., 1997). Sedimentary faunal reconstruction of late Holocene temperature record from Laurentian Slope south of Newfoundland (Marchitto and deMenocal, 2003) indicate that the late Holocene temperatures were frequently lower, mostly between 1.5 and 3.5°C, than today (~3.5°C). In the absence of analogous changes in solar activity during this interval (Fig. 3d), the distinct but step-wise overall decrease in SST of around 1.6°C from 4.9 to 2.1 kyr BP apparent in Fig. 3e, suggests a relaxation of tropical Pacific temperature gradients, weakened Hadley circulation, southward migration of ITCZ, and persistent El Niño-like pattern during the later Holocene. These conditions would have weakened the summer monsoon in subtropical Taiwan and, by extension, cultural collapses in the late Holocene, indicating

## Weak EAM intervals in Taiwan

K. Selvaraj et al.

[Title Page](#)

[Abstract](#)

[Introduction](#)

[Conclusions](#)

[References](#)

[Tables](#)

[Figures](#)

◀

▶

◀

▶

[Back](#)

[Close](#)

[Full Screen / Esc](#)

[Printer-friendly Version](#)

[Interactive Discussion](#)



a strong involvement of tropical Pacific SST in centennial-scale interglacial monsoon instability in the tropics and subtropics. Reduced tropical heat transport in the Pacific and Atlantic by warm currents, and subsequent weakness/failure of low-latitude's summer monsoon between roughly 5 and 2 kyr BP with additional impact of cold air from Siberian High must have worsened the climate then which in turn facilitated the collapse of strong civilizations evident all over the low-latitudes during this interval.

### 3.2.4 2–1.6 kyr BP event

Retreat Lake's TOC and C/N ratio records show changes in primary productivity status to in-lake algal sources (C/N=<10) around 2–1.6 kyr BP, especially at the end of lake desiccation period (Fig. 3a). Within the limits of our  $^{14}\text{C}$  chronology, this “2–1.6 kyr BP event” of weak summer monsoon in Taiwan corresponds to reduced Indian summer monsoon and increased cave aridity between 2.3 and 1.5 kyr BP recorded in Nepalese speleothem (Denniston et al., 2000) and correlates with a hiatus in Oman stalagmite between 2.7 and 1.4 kyr BP owing to weak Indian summer monsoon (Fleitmann et al., 2003) (Fig. 3c), suggesting Indo-Pacific warm pool influence via Indonesian Throughflow as well as summer monsoon in East Asia. Because the warm pool waters affect the Throughflow transportation from the Pacific to the Indian Ocean during the late Holocene when the prevailed weak trade winds throughout the Pacific could not induce strong North and South Equatorial Currents and thereby Indonesian Throughflow (Jung et al., 2004; Song et al., 2004). This interval can also be correlated with another little ice age between ~2.1 and 1.4 kyr BP and called the “Migration of Nations” (Perry and Hsu, 2000) when the Germanic tribes overran the Roman Empire and the northern Asiatic tribes overran the Chinese Empire (Hsu, 2000). This weak monsoon period further corresponds to the lowest solar activity within the Holocene, as indicated by highest  $^{10}\text{Be}$  concentrations in the atmosphere (cited in Beer, 2005) and highest ENSO activity in the tropical Pacific as shown in model studies (Clement et al., 2000; Liu et al., 2000) and coral records (Gagan et al., 2004); all indicate that ca. 2.5–1.7 kyr BP was a period of highest ENSO variability. It is apparent from the panels of Fig. 3 that tropical

## Weak EAM intervals in Taiwan

K. Selvaraj et al.

[Title Page](#)

[Abstract](#)

[Introduction](#)

[Conclusions](#)

[References](#)

[Tables](#)

[Figures](#)

◀

▶

◀

▶

[Back](#)

[Close](#)

[Full Screen / Esc](#)

[Printer-friendly Version](#)

[Interactive Discussion](#)



and subtropical drying in the Northern Hemisphere during these 4 intervals may have been responsible for the contraction of low-latitude wetlands which in turn possibly contributed to decreased methane concentrations, as was exactly noted in Greenland ice cores (Blunier et al., 1995; Alley et al., 1997).

5 Despite the coarse resolution of our proxy records, the rough correlation of weak monsoon intervals (low TOC contents and C/N ratios) with lower solar activity (higher  $\Delta^{14}\text{C}$  residuals) indicate that some, but not all, of the weak monsoon intervals are attributed to solar changes. The relationship between them appears to be relatively stronger during the periods (ca. 8.6–9.6, 8.2 and 5.5 kyr BP) of early Holocene and

10 Holocene optimum especially before 5 kyr BP under Hypsithermal condition. Their visual coincidence in the later Holocene is, however, relatively weak and that might be related either to smaller amplitudes variations of solar activity itself (Fig. 3d) or under the Neoglacial condition, the influence of ITCZ-ENSO interaction over the tropical Pacific might be vigorous and that perhaps outweighed the solar changes especially on

15 the summer EAM variability in subtropical Taiwan because of Island's proximity to the warm pool where East Asian summer monsoon originates.

#### 4 Conclusions

Lacustrine geochemical records from subtropical NE Taiwan unambiguously demonstrate four periods (~8–8.3, 5.1–5.7, 4.5–~2.1, and 2–1.6 kyr BP) of weakened summer EAM after its maximum strength ca. 8.6–7.7 kyr BP during the Holocene. Periods of weaker EAM correlate with the timings of low values of SST in the tropical Pacific, higher percentages of hematite in the North Atlantic, reduced production of North Atlantic Deep Water, and low concentrations of atmospheric methane over Greenland, suggesting a teleconnection within and between subtropical atmosphere-SST (EAM-tropical Pacific) and extratropical surface-deep water link (ice-rafted debris-NADW). Subtropical rainfall anomalies at the times of high-latitude climate change, reduced NADW formation for instance, as well as tropical Pacific SST change, reveal that mon-

#### Weak EAM intervals in Taiwan

K. Selvaraj et al.

[Title Page](#)

[Abstract](#)

[Introduction](#)

[Conclusions](#)

[References](#)

[Tables](#)

[Figures](#)

◀

▶

◀

▶

[Back](#)

[Close](#)

[Full Screen / Esc](#)

[Printer-friendly Version](#)

[Interactive Discussion](#)



soonal regions are linked to extratropical climate mainly through ocean-atmosphere interactions, especially heat and moisture transport and ENSO in the tropical Pacific. During these intervals, because of combined cooling of tropical Pacific and North Atlantic, reduced export of heat to the extratropics and atmosphere might have reduced the global wetland extent and eventually contributed to low methane to the atmosphere. It seems very probable that changes in tropical Pacific SSTs and export of water vapor to higher latitudes likely in phase with solar changes and North Atlantic climate could produce abrupt weak summer monsoon intervals in East Asia. Although South American source was called upon for the later Holocene increase of CH<sub>4</sub> in the atmosphere due to the positive hydrological effects of insolation-monsoon couple in that part of the Earth, overall covariance among diverse proxy records presented here indicates a globally well-connected postglacial monsoonal climate for the last ~8 kyr.

**Acknowledgements.** Financial support for this study was provided by the National Science Council of Taiwan (NSC-95-2621-Z-110-005 and 95-2611-M110-001).

## 15 References

Alley, R. B., Mayewski, P. A., Sowers, T., Stuiver, M., Taylor, K. C., and Clark, P. U.: Holocene climate instability: a prominent, widespread event 8200 yr ago, *Geology*, 25, 483–486, 1997.

An, Z. S., Porter, S. C., Kutzbach, J. E., Wu, X., Wang, S., Liu, X., Li, X., and Zhou, W.: Asynchronous Holocene optimum of the East Asian monsoon, *Quaternary Sci. Rev.*, 19, 743–762, 2000.

Barber, D. C., Dyke, A., Hillaire-Marcel, C., Jennings, A. E., Andrews, J. T., Kerwin, M. W., Bilodeau, G., McNeely, R., Southon, J., Morehead, M. D., and Gagnon J. M.: Forcing of the cold event of 8,200 years ago by catastrophic drainage of Laurentide lakes, *Nature*, 400, 344–348, 1999.

Bard, E., Rostek, F., and Sonzogni, C.: Interhemispheric synchrony of the last deglaciation from alkenone palaeothermometry, *Nature*, 385, 707–710, 1997.

Beer, J.: Discussion Forum: Solar variability and climate change, *Global Change NewsLetter*, 63, 18–20, 2005.

## Weak EAM intervals in Taiwan

K. Selvaraj et al.

[Title Page](#)

[Abstract](#)

[Introduction](#)

[Conclusions](#)

[References](#)

[Tables](#)

[Figures](#)

◀

▶

◀

▶

[Back](#)

[Close](#)

[Full Screen / Esc](#)

[Printer-friendly Version](#)

[Interactive Discussion](#)



Berger, A. and Loutre, M. F.: Insolation values for the climate of the last 10 million years, *Quaternary Sci. Rev.*, 10, 297–317, 1991.

Blunier, T., Chappellaz, J., Schwander, J., Stauffer, B., and Raynaud, D.: Variations in atmospheric methane concentration during the Holocene epoch, *Nature*, 374, 46–49, 1995.

5 Bond, G., Kromer, B., Beer, J., Muscheler, R., Evans, M. N., Showers, W., Hoffmann, S., Lotti-Bond, R., Hajdas, I., and Bonani, G.: Persistent solar influence on North Atlantic climate during the Holocene, *Science*, 294, 2130–2136, 2001.

Cane, M. A.: A role for the tropical Pacific, *Science*, 282, 59–61, 1998.

10 Chen, C. T. A., Lan, H. C., Lou, J. Y., and Chen, Y. C.: The dry Holocene Megathermal in Inner Mongolia, *Palaeogeogr. Palaeoocl.*, 193, 181–200, 2003.

Clement, A. C., Seager, R., and Cane, M. A.: Suppression of El Niño during the mid-Holocene by changes in the Earth's orbit, *Paleoceanography*, 15, 731–737, 2000.

15 Cullen, H. M., deMenocal, P. B., Hemming, S., Hemming, G., Brown, F. H., Guilderson, T., and Sirocko, F.: Climate change and the collapse of the Akkadian empire: evidence from the deep sea, *Geology*, 28, 379–382, 2000.

Dahl-Jensen, D., Mosegaard, K., Gundestrup, G., Clow, G. D., Johnson, S. J., Hansen, A. W., and Balling, B.: Past temerature directly from the Greenland ice sheet, *Science*, 282, 268–271, 1998.

20 deMenocal, P. B., Ortiz, J., Guilderson, T., Adkins, J., Sarnthein, M., Baker, L., and Yarusinsky, M.: Abrupt onset and termination of the African Humid Period: rapid climate responses to gradual insolation forcing, *Quaternary Sci. Rev.*, 19, 347–361, 2000.

Denniston, R. F., González, L. A., Asmerom, Y., Sharma, R. H., and Reagan, M. K.: Speleothem evidence for changes in Indian summer monsoon precipitation over the last ~2300 years, *Quaternary Res.*, 53, 196–202, 2000.

25 Enzel, Y., Ely, L. L., Mishra, S., Ramesh, R., Amit, R., Lazar, B., Rajaguru, S. N., Baker, V. R., and Sandler, A.: High-resolution Holocene environmental changes in the Thar Desert, northwestern India, *Science*, 284, 125–128, 1999.

Fleitmann, D., Burns, S. J., Mudelsee, M., Neff, U., Kramers, J., Mangini, A., and Matter, A.: Holocene forcing of the Indian monsoon recorded in a stalagmite from Southern Oman, *Science*, 300, 1737–1739, 2003.

30 Fleitmann, D., Burns, S. J., Mangini, A., Mudelsee, M., Kramers, J., Villa, I., Neff, U., Al-Subbary, A. A., Buettner, A., Hippler, D., and Matter, A.: Holocene ITCZ and Indian monsoon dynamics recorded in stalagmites from Oman and Yemen (Socotra), *Quaternary Sci. Rev.*,

## Weak EAM intervals in Taiwan

K. Selvaraj et al.

[Title Page](#)

[Abstract](#)

[Introduction](#)

[Conclusions](#)

[References](#)

[Tables](#)

[Figures](#)

◀

▶

◀

▶

[Back](#)

[Close](#)

[Full Screen / Esc](#)

[Printer-friendly Version](#)

[Interactive Discussion](#)



Gagan, M. K., Hendy, E. J., Haberle, S. G., and Hantoro, W. S.: Post-glacial evolution of the Indo-Pacific Warm Pool and El Niño-Southern Oscillation, *Quaternary Int.*, 118–119, 127–143, 2004.

5 Gupta, A. K., Anderson, D. M., and Overpeck, J. T.: Abrupt changes in the Asian southwest monsoon during the Holocene and their links to the North Atlantic Ocean, *Nature*, 421, 354–357, 2003.

Gupta, A. K., Das, M., and Anderson, D. M.: Solar influence on the Indian summer monsoon during the Holocene, *Geophys. Res. Lett.*, 32, L17703, doi:10.1029/2005GL022685, 2005.

10 Haug, G. H., Hughen, K. A., Sigman, D. M., Peterson, L. C., and Röhli, U.: Southward migration of the intertropical convergence zone through the Holocene, *Science*, 293, 1304–1308, 2001.

Hodell, D. A., Kanfoush, S. L., Shemesh, A., Crosta, X., Charles, C. D., and Guilderson, T. P.: Abrupt cooling of Antarctic surface waters and sea ice expansion in the South Atlantic sector 15 of the Southern Ocean at 5000 cal yr B.P., *Quaternary Res.*, 56, 191–198, 2001.

Hsu, K. J.: *Climate and Peoples: A Theory of History*, Orell Fussli, Zurich, 2000.

Indermühle, A., Stocker, T. F., Joos, F., Fischer, H., Smith, H. J., Wahnen, M., Deck, B., Mastrianni, D., Tschumi, J., Blunier, T., Meyer, R., and Stauffer, B.: Holocene carbon-cycle dynamics based on CO<sub>2</sub> trapped in ice at Taylor Dome, Antarctica, *Nature*, 398, 121–126, 20 1999.

Jian, Z., Wang, P., Saito, Y., Wang, J., Pflauman, U., Oba, T., and Cheng, X.: Holocene variability of the Kuroshio Current in the Okinawa Trough, northwestern Pacific Ocean, *Earth Planet. Sci. Lett.*, 184, 305–319, 2000.

Joussaume, S., Taylor, K. E., Braconnot, P., et al.: Monsoon changes for 6000 years ago: 25 results of 18 simulations from the Paleoclimate Modeling Intercomparison Project (PMIP), *Geophys. Res. Lett.*, 26, 859–862, 1999.

Jung, S. J. A., Davies, G. R., Ganssen, G. M., and Kroon, D.: Synchronous Holocene sea surface temperature and rainfall variations in the Asian monsoon system, *Quaternary Sci. Rev.*, 23, 2207–2218, 2004.

Kutzbach, J. E. and Otto-Bliesner, B. I.: The sensitivity of the African-Asian monsoonal climate 30 to orbital parameter changes for 9000 yr B.P. in a low-resolution general circulation model, *J. Atmospheric Sci.*, 39, 1177–1188, 1982.

Lea, D. W., Pak, D. K., and Spero, H. J.: Climate impact of late Quaternary Equatorial Pacific

## Weak EAM intervals in Taiwan

K. Selvaraj et al.

[Title Page](#)

[Abstract](#)

[Introduction](#)

[Conclusions](#)

[References](#)

[Tables](#)

[Figures](#)

◀

▶

◀

▶

[Back](#)

[Close](#)

[Full Screen / Esc](#)

[Printer-friendly Version](#)

[Interactive Discussion](#)



sea surface temperature variations, *Science*, 289, 1719–1724, 2000.

Liew, P. M., Lee, C. Y., and Kuo, C. M.: Holocene thermal optimal and climate variability of East Asian monsoon inferred from forest reconstruction of a subalpine pollen sequence, Taiwan, *Earth Planet. Sci. Lett.*, 250, 596–605, 2006.

5 Liu, K. B., Yao, Z., and Thompson, L. G.: A pollen record of Holocene climatic changes from the Dunde ice cap, Qinghai-Tibetan Plateau, *Geology*, 26, 135–138, 1998.

Liu, Z., Kutzbach, J., and Wu, L.: Modeling climate shift of El Niño variability in the Holocene, *Geophys. Res. Lett.*, 27, 2265–2268, 2000.

Lou, J. Y. and Chen, C. T. A.: Paleoclimatological and paleoenvironmental records since 4000 10 a B.P. in sediments of alpine lakes in Taiwan, *Sci. China Ser. D*, 40, 424–431, 1997.

Marchitto, T. M. and deMenocal, P. B.: Late Holocene variability of upper North Atlantic Deep Water temperature and salinity, *Geochem. Geophys. Geosys.*, 4, 1100, doi:10.1029/2003GC000598, 2003.

15 Mayewski, P. A., Rohling, E. E., Stager, J. C., Karlén, W., Maasch, K. A., Meeker, L. D., Meyerson, E. A., Gasse, F., van Kreveld, S., Holmgren, K., Lee-Thorp, J., Rosqvist, G., Rack, F., Staubwasser, M., Schneider, R. R., and Steig, E. J.: Holocene climate variability, *Quaternary Res.*, 62, 243–255, 2004.

McDermott, F., Matthey, D. P., and Hawkesworth, C.: Centennial-scale Holocene climate variability revealed by a high-resolution speleothem  $\delta^{18}\text{O}$  record from SW Ireland, *Science*, 294, 20 1328–1331, 2001.

Meyers, P. A. and Lallier-Vergès, E.: Lacustrine sedimentary organic matter records of late Quaternary paleoclimates, *J. Paleolimnology*, 21, 345–372, 1999.

Morrill, C., Overpeck, J. T., and Cole, J. E.: A synthesis of abrupt changes in the Asian summer monsoon since the last deglaciation, *The Holocene*, 13, 465–476, 2003.

25 Morrill, C., Overpeck, J. T., Cole, J. E., Liu, K., Shen, C., and Tang, L.: Holocene variations in the Asian monsoon inferred from the geochemistry of lake sediments in central Tibet, *Quaternary Res.*, 65, 232–243, 2006.

O'Brien, S. R., Mayewski, P. A., Meeker, L. D., Meese, D. A., Twickler, M. S., and Whitlow, S. I.: Complexity of Holocene climate as reconstructed from a Greenland ice core, *Science*, 270, 30 1962–1964, 1995.

Oppo, D. W., McManus, J. F., and Cullen, J. L.: Deepwater variability in the Holocene epoch, *Nature*, 422, 277–278, 2003.

Palmer, T. N. and Mansfield, D. A.: Response of two atmospheric general circulation models

## Weak EAM intervals in Taiwan

K. Selvaraj et al.

[Title Page](#)

[Abstract](#)

[Introduction](#)

[Conclusions](#)

[References](#)

[Tables](#)

[Figures](#)

◀

▶

◀

▶

[Back](#)

[Close](#)

[Full Screen / Esc](#)

[Printer-friendly Version](#)

[Interactive Discussion](#)



to sea-surface temperature anomalies in the tropical East and West Pacific, *Nature*, 310, 483–485, 1984.

CPD

4, 929–953, 2008

Perry, C. A. and Hsu, K. J.: Geophysical, archaeological, and historical evidence support a solar-output model for climate change, *Proc. Nat. Aca. Sci.*, 97, 12 433–12 438, 2000.

5 Poore, R. Z., Dowsett, H. J., and Verardo, S.: Millennial- to century-scale variability in Gulf of Mexico Holocene climate records, *Paleoceanography*, 18, 1048, doi:10.1029/2002PA000868, 2003.

Porter, S. C.: Onset of Neoglaciation in the Southern Hemisphere, *J. Quaternary Sci.*, 15, 395–408, 2000.

10 Porter, S. C. and Zhou, W. J.: Synchronism of Holocene East Asian monsoon variations and North Atlantic drift-ice tracers, *Quaternary Res.*, 65, 443–449, 2006.

Rind, D.: Puzzles from the tropics, *Nature*, 346, 317–318, 1990.

Rodbell, D. T., Seltzer, G. O., Anderson, D. M., Abbott, M. B., Enfield, D. B., and Newman, J. H.: An ~15,000-year record of El Niño-driven alleviation in southwestern Ecuador, *Science*, 283, 516–520, 1999.

15 Rohling, E. J. and Pälike, H.: Centennial-scale climate cooling with a sudden cold event around 8,200 years ago, *Nature*, 434, 975–979, 2005.

Sandweiss, D. H., Richardson, J. B., Reitz, E. J., Rollins, H. B., and Maasch, K. A.: Geoarchaeological evidence from Peru for a 5000 B.P. onset of El Niño, *Science*, 273, 1531–1533, 1996.

20 Selvaraj, K. and Chen, C. T. A.: Moderate chemical weathering of subtropical Taiwan: Constraints from solid-phase geochemistry of sediments and sedimentary rocks, *J. Geology*, 114, 101–116, 2006.

Selvaraj, K., Chen, C. T. A., and Lou, J. Y.: Holocene East Asian monsoon variability: links to solar and tropical Pacific forcing, *Geophys. Res. Lett.*, 34, L01703, doi:10.1029/2006GL028155, 2007.

25 Song, Q., Gordon, A. L., and Visbeck, M.: Spreading of the Indonesian Throughflow in the Indian Ocean, *J. Physical Oceanogr.*, 34, 772–792, 2004.

Steig, E. J.: Mid-Holocene climate change, *Science*, 286, 1485–1487, 1999.

30 Stott, L., Poulsen, C., Lund, S., and Thunell, R.: Super ENSO and global climate oscillations at millennial time scales, *Science*, 297, 222–226, 2002.

Stott, L., Cannariato, K., Thunell, R., Haug, G. H., Koutavas, A., and Lund, S.: Decline of surface temperature and salinity in the western tropical Pacific Ocean in the Holocene epoch,

## Weak EAM intervals in Taiwan

K. Selvaraj et al.

[Title Page](#)

[Abstract](#)

[Introduction](#)

[Conclusions](#)

[References](#)

[Tables](#)

[Figures](#)

◀

▶

◀

▶

[Back](#)

[Close](#)

[Full Screen / Esc](#)

[Printer-friendly Version](#)

[Interactive Discussion](#)



Nature, 431, 56–59, 2004.

Street-Perrott, F. A. and Perrott, R. A.: Abrupt climate fluctuations in the tropics: the influence of Atlantic Ocean circulation, *Nature*, 343, 607–612, 1990.

5 Stuiver, M. and Grootes, P. M.: GISP2 oxygen isotope ratios, *Quaternary Res.*, 53, 277–284, 2000.

Stuiver, M., Reimer, P. J., Bard, E., Beck, J. W., Burr, G. S., Hughen, K. A., Kromer, B., McCormac, G., Plicht, J. V. D., and Spurk, M.: INTCAL98 Radiocarbon age calibration, 24,000-0 cal BP, *Radiocarbon*, 40, 1041–1083, 1998.

10 Wang, L., Sarnthein, M., Erlenkeuser, H., Grimalt, J., Grootes, P. M., Heiling, S., Ivanova, E., Kienast, M., Pelejero, C., and Plaumann, U.: East Asian monsoon climate during the late Pleistocene: high-resolution sediment records from the South China Sea, *Mar. Geol.*, 156, 245–284, 1999.

15 Wang, Y. J., Cheng, H., Edwards, R. L., He, Y., Kong, X., An, Z. S., Wu, J., Kelly, M. J., Dykoski, C. A., and Li, X.: The Holocene Asian monsoon: links to solar changes and North Atlantic climate, *Science*, 308, 854–857, 2005.

Wei, K. Y. and Gasse, F.: Oxygen isotopes in lacustrine carbonates of West China revisited: implications for post glacial changes in summer monsoon circulation, *Quaternary Sci. Rev.*, 18, 1315–1334, 1999.

20 Wei, K. Y., Yang, T. N., and Huang, C. Y.: Glacial-Holocene calcareous nannofossils and paleoceanography in the northern South China Sea, *Mar. Micropaleontology*, 32, 95–114, 1997.

Weiss, H., Courty, M. A., Wetterstrom, W., Guichard, F., Senior, L., Meadow, R., and Crunow, A.: The genesis and collapse of third millennium north Mesopotamian civilization, *Science*, 261, 995–1004, 1993.

25 Wu, W. and Liu, T.: Possible role of the “Holocene Event 3” on the collapse of Neolithic Cultures around the Central Plain of China, *Quaternary Int.*, 117, 153–166, 2004.

CPD

4, 929–953, 2008

---

## Weak EAM intervals in Taiwan

K. Selvaraj et al.

---

[Title Page](#)

[Abstract](#)

[Introduction](#)

[Conclusions](#)

[References](#)

[Tables](#)

[Figures](#)

◀

▶

◀

▶

[Back](#)

[Close](#)

[Full Screen / Esc](#)

[Printer-friendly Version](#)

[Interactive Discussion](#)



**Weak EAM intervals  
in Taiwan**

K. Selvaraj et al.

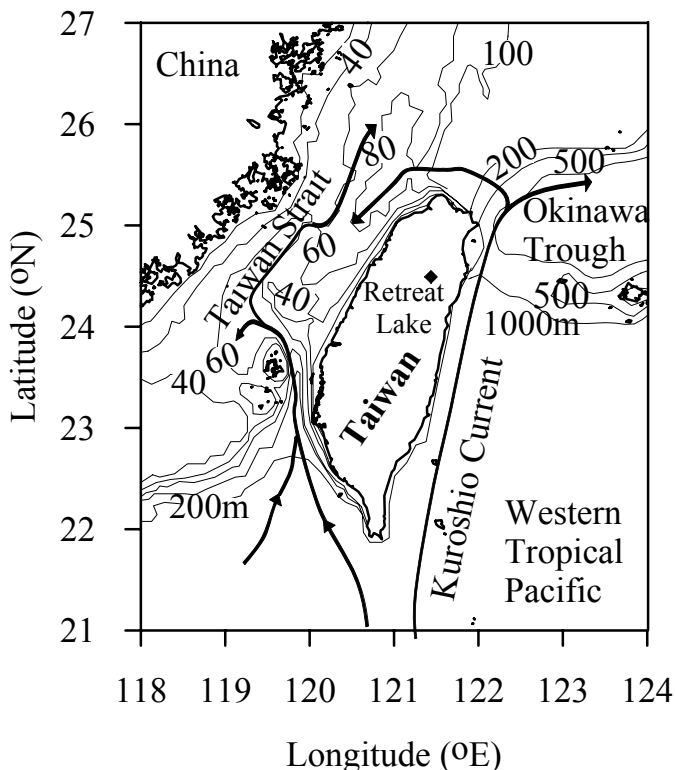


**Fig. 1.** Map showing the study area, Retreat Lake, and the main path of warm Kuroshio Current in the western tropical Pacific and Taiwan Strait. The depth contours are in meters.

<a href="#">Title Page</a>	
<a href="#">Abstract</a>	<a href="#">Introduction</a>
<a href="#">Conclusions</a>	<a href="#">References</a>
<a href="#">Tables</a>	<a href="#">Figures</a>
<a href="#">◀</a>	<a href="#">▶</a>
<a href="#">◀</a>	<a href="#">▶</a>
<a href="#">Back</a>	<a href="#">Close</a>
<a href="#">Full Screen / Esc</a>	

[Printer-friendly Version](#)[Interactive Discussion](#)

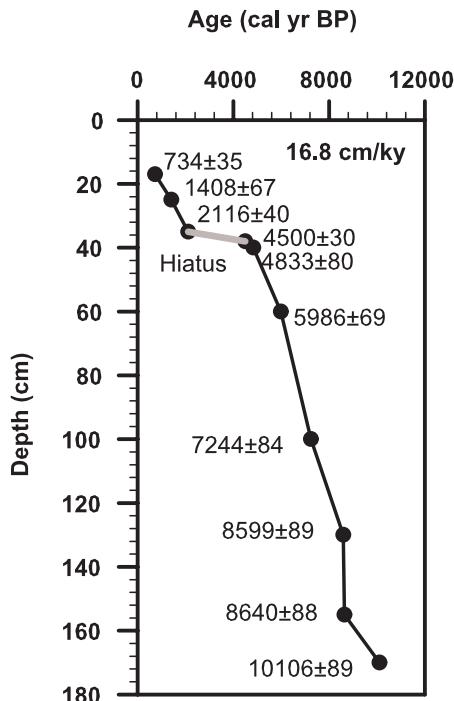


**Fig. 2.** Calibrated calendar ages versus depth in the sediment core of Retreat Lake showing the Holocene mean sedimentation rate of 16.8 cm/kyr (data taken from Selvaraj et al., 2007).

## Weak EAM intervals in Taiwan

K. Selvaraj et al.

[Title Page](#)

[Abstract](#)

[Introduction](#)

[Conclusions](#)

[References](#)

[Tables](#)

[Figures](#)

◀

▶

◀

▶

[Back](#)

[Close](#)

[Full Screen / Esc](#)

[Printer-friendly Version](#)

[Interactive Discussion](#)



## Weak EAM intervals in Taiwan

K. Selvaraj et al.

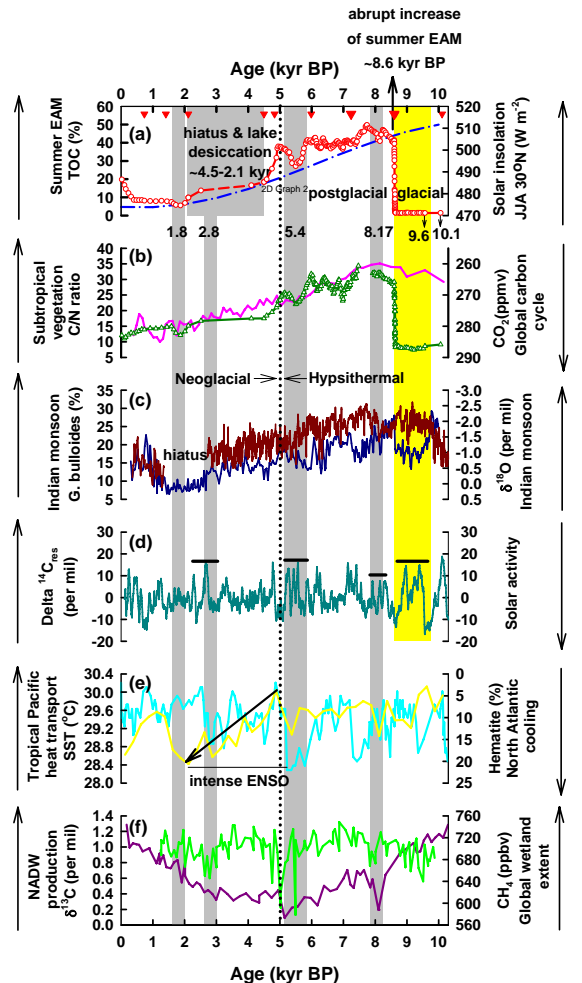


Fig. 3.

**Fig. 3.** Weak summer East Asian monsoon (EAM) intervals in subtropical Taiwan (grey bars) compared with Northern Hemisphere summer insolation and other Holocene climate records. Panel **(a)** shows Retreat Lake's total organic carbon (TOC) record (red) and insolation curve (blue) at 30° N, averaged from June to August (JJA) (Berger and Loutre, 1991); low TOC values indicate weak summer EAM precipitation in Taiwan. Panel **(b)** presents Retreat Lake's C/N ratio record (dark green) and atmospheric CO<sub>2</sub> record (pink) from the Taylor Dome ice core, Antarctica (Indermühle et al., 1999); low C/N ratio indicates decreased subtropical vegetation and high CO<sub>2</sub> is a likely effect of reduced low-latitude's vegetation during the later Holocene. Panel **(c)** illustrates *Globigerina bulloides* percentage (dark blue) in Hole 723A (Gupta et al., 2005) and Qunf cave  $\delta^{18}\text{O}$  record (dark red) (Fleitmann et al., 2003); higher faunal abundance and higher negative isotope values reveal stronger Indian summer monsoon. Panel **(d)** depicts atmospheric  $\Delta^{14}\text{C}_{\text{residuals}}$  record (dark cyan) (Stuiver et al., 1998); higher  $\Delta^{14}\text{C}_{\text{res}}$  indicate weak solar winds and irradiance. Panel **(e)** gives sea surface temperature (SST) record (yellow) from the tropical Pacific core MD81 (Stott et al., 2004) and hematite percentages in core VM29-191 (cyan) from the North Atlantic (Bond et al., 2001); low SSTs reflect the relatively reduced heat and moisture transport to the marginal seas and northern North Pacific and high percentages of hematite reflect the cool North Atlantic. Panel **(f)** shows benthic foraminifera  $\delta^{13}\text{C}$  record (light green) from ODP site 980, sub-polar northeastern Atlantic (Oppo et al., 2003) and CH<sub>4</sub> record from the Greenland ice core GRIP (Blunier et al., 1995); low carbon isotope values indicate reduced North Atlantic Deep Water production and low concentrations of CH<sub>4</sub> reveal reduced extent of global wetland. Also shown are ages for an abrupt increase of the postglacial summer EAM (~8.6 kyr BP; Selvaraj et al., 2007) and the period of “lake desiccation” (~4.5–2.1 kyr BP) in subtropical Taiwan. Red triangles in the top panel represent the <sup>14</sup>C ages. Yellow bar highlights the insolation-monsoon relationship during the early Holocene and dotted line runs through all panels at 5 kyr BP represents the Hypsithermal-Neoglacial transition.

## Weak EAM intervals in Taiwan

K. Selvaraj et al.

[Title Page](#)

[Abstract](#)

[Introduction](#)

[Conclusions](#)

[References](#)

[Tables](#)

[Figures](#)

◀

▶

◀

▶

[Back](#)

[Close](#)

[Full Screen / Esc](#)

[Printer-friendly Version](#)

[Interactive Discussion](#)

